Anisotropic Thermal Diffusivity and Conductivity of YBCO(123) and YBCO(211) Mixed Crystals. II

1994 Jpn. J. Appl. Phys. 33 6157

(http://iopscience.iop.org/1347-4065/33/11R/6157)

Jpn. J. Appl. Phys. Vol. 33 (1994) pp. 6157-6159
Part 1, No. 11, November 1994

Anisotropic Thermal Diffusivity and Conductivity of YBCO(123) and YBCO(211) Mixed Crystals. II

Manabu IKEBE, Hiroyuki FUJISHIRO, Tomoyuki NAITO, Michiaki MATSUKAWA and Koshichi NOTO
Department of Materials Science and Technology, Faculty of Engineering, Iwate University, 4-3-5 Ueda, Morioka 020

(Received May 31, 1994; accepted for publication September 17, 1994)

The electron and phonon contributions to the thermal conductivity and diffusivity of the $YBa_2Cu_3O_{7-x}$ (YBCO(123)) matrix phase in the mixed crystal were separated by use of the Kadanoff theory. The phonon mean free path l_{ph} and the phonon relaxation time τ_{ph} were determined. The phonon thermal conductivity and diffusivity were analyzed based on the Tewordt and Wölkhausen theory to estimate the electron-phonon coupling parameter λ and the strength of the various phonon scattering mechanisms.

KEYWORDS: Y-Ba-Cu-O superconductor, thermal diffusivity, thermal conductivity, specific heat, phonon mean free path, phonon relaxation time, phonon scattering mechanisms

1. Introduction

In a previous paper,[1] we discussed the effect of the Y_2BaCuO_5 (YBCO(211)) particles on the thermal properties of YBCO mixed crystals prepared by modified melt texture growth (MMTG).[2,3] We estimated the *ab*-plane and *c*-axis thermal conductivity of the $YBa_2Cu_3O_{7-x}$ (123) matrix phase based on a simple model.[4] In this paper, II, we separate the electron and phonon contributions to conductivity κ and diffusivity α. Assuming that the phonon is the main heat carrier in the entire temperature range, we attempt to explain the characteristic enhancement of in-plane κ and α below T_c based on the Tewordt and Wölkhausen (TW)[5] theory and estimate the electron phonon coupling parameter λ. Although several conflicting opinions have been presented[6-9] for the possible origin of κ enhancement, strong support for the phonon as the main heat carrier may be provided if the behavior of κ and α can be explained in a systematic manner by the TW theory.

2. Results and Discussion

The temperature dependence of the electrical resistivity of the YBCO mixed crystals prepared by MMTG is shown in Fig. 1, which presents both the *ab*-plane resistivity $\rho_{ab}(T)$ of sample #1 and the *c*-direction resistivity $\rho_c(T)$ of sample #2 (samples #1 and #2 are described in Paper I). Both ρ_{ab} and ρ_c show a sharp superconducting transition near T_c=90 K. It is notable that the anisotropy of resistivity is very large and ρ_c/ρ_{ab} exceeds 100 over the whole temperature range. In order to estimate the electron contribution to the thermal conductivity κ_{ab}^{123} of the (123) phase, we must determine the correct value of the electrical resistivity of the (211) phase. ρ_{ab}^{123} is estimated based on the same model as used in Paper I. Because the present YBCO specimens contain the almost completely insulating (211) phase, the inner (211)-phase cube in Fig. 8 in Paper I can be replaced by a corresponding cubic void. In Fig. 2 we plot the conductivity of the model cube containing the smaller cubic void as a function of the porosity $P(=\Delta V/V)$, where V is the volume of the sample cube and ΔV is the volume of the cubic void, respectively. We can see in Fig. 2 that at P=0.286, which corresponds to the volume fraction of the (211) phase in the present mixed crystal, the observed conductivity should be reduced by a factor of 0.68. We assume that the correct ρ_{ab}^{123} value is obtained by multiplying the

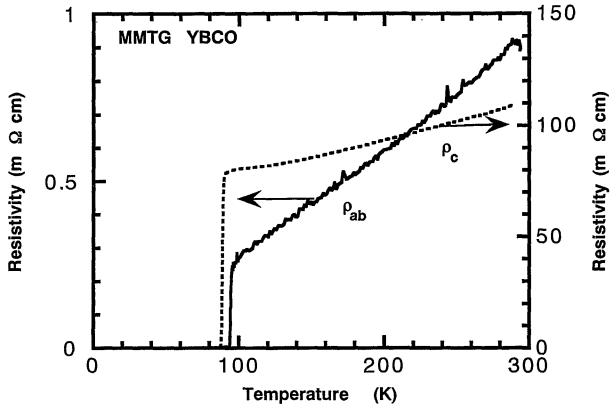

Fig. 1. The temperature dependence of the electrical resistivity of the MMTG samples in the *ab*-plane (ρ_{ab}, sample #1) and along the *c*-axis (ρ_c, sample #2).

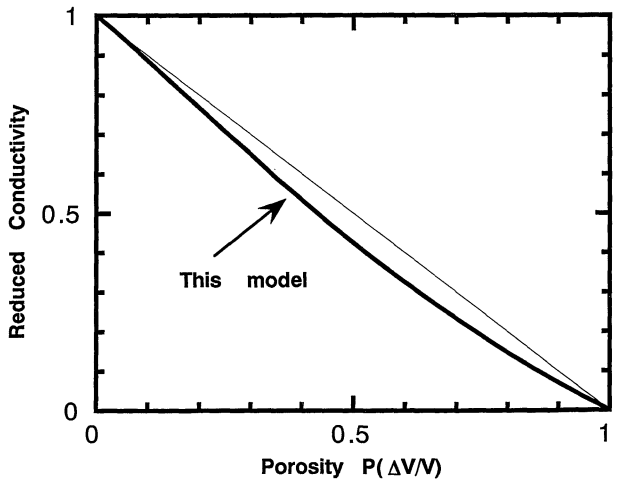

Fig. 2. The reduced conductivity as a function of porosity P for the model cube containing a smaller cubic void which is shown in Fig. 8 in Paper I.

measured ρ_{ab} by this factor. After this correction for $\rho_{ab}^{123}(T)$, the electron contribution to the thermal conductivity is estimated by use of the Wiedemann-Franz law above T_c and by use of the following modified Kadanoff expression[10] below T_c:

$$\frac{\kappa_{es}}{\kappa_{en}}=\frac{3}{2\pi^2}\int_0^\infty d\varepsilon\varepsilon^2\,\mathrm{sech}^2\left\{\frac{1}{2}[\varepsilon^2+(\beta\Delta)^2]^{1/2}\right\}\frac{\left[1+\boldsymbol{a}\frac{T}{T_c}\right]}{\left[\frac{\varepsilon}{\{\varepsilon^2+(\beta\Delta)^2\}^{1/2}}+\boldsymbol{a}\frac{T}{T_c}\right]}. \quad (1)$$

Here, $\boldsymbol{a}$ represents the ratio of the phonon electrical resistance at T_c and the residual impurity electrical resistance ($\boldsymbol{a}$ was set equal to 100 assuming predominant T-linear resistance for the present sample), ε is the electron energy relative to the chemical potential, Δ the BCS energy gap and β is $1/k_BT$. By subtracting the estimated electron contribution κ_{eab}^{123} from κ_{ab}^{123} in Paper I, we obtain the phonon contribution κ_{gab}^{123}. These estimated κ_{eab}^{123} and κ_{gab}^{123} values are plotted in Fig. 3 together with the total κ_{ab}^{123} obtained in Paper I.

In Usual metals, phonons are scattered mainly by conduction electrons and, to a lesser extent, by various crystal defects and grain boundaries. For oxide superconductors, it is also desirable to determine the strength of electron-phonon coupling in connection with the origin of the superconductivity in this system. Tewordt and Wölkhausen (TW)[5] have analyzed the phonon thermal conductivity of the oxide superconductors and estimated the electron-phonon coupling parameter λ. According to TW, the phonon thermal conductivity follows the formula

$$\kappa_g=\frac{3\,dnRT^3v^2}{M\Theta_D^3}\int_0^{\Theta_D/T}\frac{x^4e^x}{(e^x-1)^2}\tau_{ph}\,dx, \quad (2)$$

where x is the reduced phonon frequency, n the number of atoms composing one molecule of the compound, R the gas constant, Θ_D the Debye temperature, v the sound velocity, d the mass density and M the mass of 1 mole of the compound. The phonon relaxation time τ_{ph} is given by

$$\frac{1}{\tau_{ph}}=\tau_b^{-1}+sT^2x^2+pT^4x^4+ETxg. \quad (3)$$

Here, τ_b is the phonon relaxation time due to grain boundaries and s, p and E refer to the strength of phonon scattering by sheetlike faults, point defects and electrons, respectively. The ratio of phonon-electron scattering in the normal and superconducting states, τ_{phn}/τ_{phs}, is given by the function $g(x, y)$ which depends on the energy gap through the parameter $y=\Delta(T)/k_BT$. The BCS value of $\Delta(T)$ was assumed in the present analyses. The exact form of $g(x, y)$ was given by Bardeen, Rickayzen and Tewordt (BRT).[11] By using $g(x, y)$ taken from BRT, we implicitly assume s-wave symmetry for the energy gap $\Delta(T)$.

In order to perform fitting on the basis of eqs. (2) and (3), we need the value of Θ_D, which was determined to be $\Theta_D=440$ K from the specific heat values, C_{ab}^{123} and C_c^{123}, estimated in Paper I assuming the following Debye formula,

$$C=9nR\frac{T^3}{\Theta_D^3}\int_0^{\Theta_D/T}\frac{x^4e^x}{(e^x-1)^2}\,dx. \quad (4)$$

The examples of the Debye fitting curve are shown in Fig. 4.

With the use of this Θ_D value, the best-fit curve for the in-plane phonon thermal conductivity κ_{gab}^{123} was obtained with the parameter values in Table I. The fitting curve is presented in Fig. 3. Since the electrons which condensed in the ground state do not scatter phonons, $g(x, y)=\tau_{phn}/\tau_{phs}$ approaches zero below T_c, and κ_{gab}^{123} shows a characteristic upturn and bump with decreas-

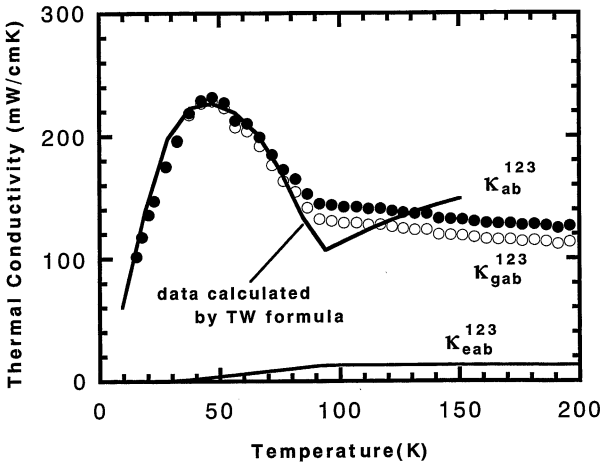

Fig. 3. The temperature dependence of the thermal conductivity κ_{ab}^{123} (●), the electron contribution κ_{eab}^{123} estimated by the WF law and Kadanoff formula and the phonon contribution κ_{gab}^{123} (○) given by $\kappa_{gab}^{123}=\kappa_{ab}^{123}-\kappa_{eab}^{123}$. The solid line is the calculated curve based on the TW-BRT theory using parameter values in Table I.

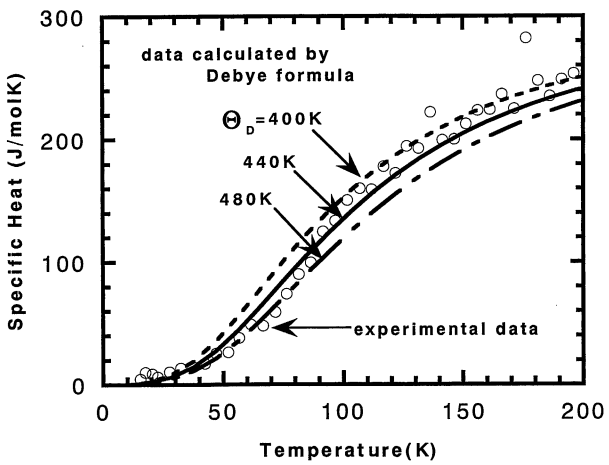

Fig. 4. The Debye fitting curves for the specific heat C_{ab}^{123} of the (123) phase estimated from κ_{ab}^{123} and α_{ab}^{123}.

Table I. Characteristic parameters of the YBCO (123) phase.

d (g/cm^3)	5.94
M (g/mol)	666
τ_b^{-1}(s^{-1})	5.3×10^7
p (K^{-4} s^{-1})	10
s (K^{-2} s^{-1})	1.2×10^6
E (K^{-1} s^{-1})	9.9×10^8
λ	0.40
Θ_D (K)	440
v (m/s)	3110

ing temperature. The electron-phonon coupling parameter λ is related to the E value in eq. (3) by the following formula:[5]

$$\lambda \approx \frac{2a\langle t\rangle E}{\pi v}, \tag{5}$$

where a is the average of the lattice constant and $\langle t\rangle$ is the effective hopping matrix element for a two-dimensional band of electrons. if we use the values of $a=4$ Å and $\langle t\rangle=5000$ K following TW and set $v=3110$ m/s,[12] then we obtain $\lambda=0.40$ for the (123) phase of the present crystal.

Since we have already separated the electron and phonon contributions to the in-plane conductivity, the separation of the two contributions to the diffusivity can be done in a similar manner. We define the phonon thermal diffusivity α_g by

$$\alpha_g=\frac{\kappa_g}{C_{ph}}=\frac{1}{3}v^2\tau_{ph}=\frac{1}{3}vl_{ph}. \tag{6}$$

The electron contribution to the specific heat is very small in the temperature range studied, and we approximate α_g of the YBCO (123) phase in the ab-plane and in the c-direction by

$$\alpha_{gab}^{123}=\frac{\kappa_{gab}^{123}}{C_{ab}^{123}}, \tag{7}$$

and

$$\alpha_{gc}^{123}=\frac{\kappa_{gc}^{123}}{C_{c}^{123}}. \tag{8}$$

If we use the value $v=3110$ m/s,[12] the phonon mean free path l_{ph} and the scattering time τ_{ph} can be determined, as shown in Fig. 5. In the case of α_{gc}^{123}, α_c^{123} determined in Paper I can be regarded as α_{gc}^{123} since the electron contribution to κ_c^{123} is quite small owing to the very large ρ_c.

3. Conclusions

The phonon and electron contributions to the in-plane thermal conductivity κ_{ab}^{123} and diffusivity α_{ab}^{123} were separated for the $YBa_2Cu_3O_{7-X}$ matrix phase in the YBCO (123) and YBCO (211) mixed crystals. The in-plane thermal conductivity and diffusivity were analyzed on the basis of the Tewordt and Wölkhausen theory, assuming the phonon to be the main thermal carrier both above and below T_c. Agreement between the theory and experimental results is satisfactory, which supports our assumption and indicates that the enhancement in κ_{ab}^{123} below T_c is due to phonons. The electron-phonon coupling parameter λ is estimated to be ≈0.40. The phonon scattering strength due to various crystal defects was also estimated. The phonon mean free path l_{ph} and the phonon scattering time τ_{ph} were determined as function of temperature from the estimated phonon thermal diffusivities both in the ab-plane and in the c-direction.

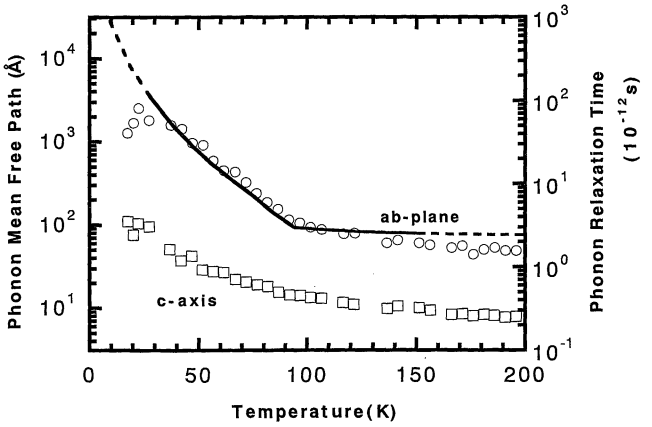

Fig. 5. The phonon mean free path (left-hand ordinate) and phonon relaxation time (right-hand ordinate) as a function of temperature. The estimated α_{gab}^{123} is presented by ○. The solid line represents the fitting curve for α_{gab}^{123}, which was calculated by use of the TW theory for κ_{gab}^{123} and the Debye theory for C_{ab}^{123}. α_c^{123} data (□) are also shown for comparison.

In the present analyses, we assumed s-wave coupling of the order parameter $\Delta(T)$. Preliminary analyses suggest that similarly good or somewhat better agreement can be achieved by applying the d-wave coupling model[13] for $\kappa_{ab}^{123}(T)$ and $\alpha_{ab}^{123}(T)$. In order to arrive at an unambiguous conclusion, however, the experiment must be extended to the lower temperature range with improved precision for $\alpha(T)$ measurement on a single-phase crystal. Such studies are under way.

1) H. Fujishiro, M. Ikebe, T. Naito, K. Noto, S. Kohayashi and S. Yoshizawa: Jpn. J. Appl. Phys. **33** (1994) 4971.
2) S. Kohayashi, Y. Ishikawa, S. Yoshizawa and H. Kojima: *Proc. Int. Superconducting Symp. (ISS) '92* (Springer-Verlag, Tokyo, 1993) p. 795.
3) K. Tenya, H. Miyajima, Y. Ishikawa, S. Kohayashi and S. Yoshizawa: J. Mag. Soc. Jpn. **16** (1992) 467.
4) M. Ikebe, H. Fujishiro, T. Naito, K. Noto, S. Kohayashi and S. Yoshizawa: Cryogenics **34** (1994) 57.
5) L. Tewordt and T. Wölkhausen: Solid State Commun. **70** (1989) 839.
6) S. D. Peacor, R. A. Richardson, F. Nori and C. Uher: Phys. Rev. B **44** (1991) 9508.
7) R. C. Yu, M. B. Salamon, J. P. Lu and W. C. Lee: Phys. Rev. Lett. **69** (1992) 1431.
8) J. L. Cohn, V. Z. Kresin, M. E. Reeves and S. A. Wolf: Phys. Rev. Lett. **71** (1993) 1657.
9) O. Klein: Phys. Rev. Lett. **72** (1994) 1390.
10) L. P. Kadanoff and P. C. Martin: Phys. Rev. **124** (1962) 670.
11) J. Bardeen, G. Rickayzen and L. Tewordt: Phys. Rev. **113** (1959) 982.
12) Y. Horie, Y. Terashi, H. Fukuda, T. Fukami and S. Mase: Solid State Commun. **64** (1987) 501.
13) L. Tewordt and T. Wölkhausen: Solid State Commun. **75** (1990) 515.